

Evolution of half plateaus as a function of electric field in a ballistic quasi-one-dimensional constriction

N. K. Patel, J. T. Nicholls, L. Martín-Moreno, M. Pepper, J. E. F. Frost, D. A. Ritchie, and
G. A. C. Jones

Cavendish Laboratory, Madingley Road, Cambridge, CB3 0HE, United Kingdom

(Received 22 July 1991)

We have investigated the effect of applying a dc source-drain voltage across a quasi-one-dimensional constriction formed at a GaAs-Al_xGa_{1-x}As heterojunction. For conductances greater than $2e^2/h$, the measurements can be compared with the predictions of an adiabatic model proposed by Glazman and Khaetskii, in which the voltage is dropped symmetrically across the one-dimensional constriction. The source-drain voltage measurements are used to obtain the subband energies of the quasi-one-dimensional constriction. For conductances less than $2e^2/h$, the Glazman-Khaetskii model is no longer applicable and anomalous structure is observed.

I. INTRODUCTION

By using a split gate, it is possible¹ to define a narrow constriction in the two-dimensional electron gas (2DEG) formed at a GaAs-Al_xGa_{1-x}As heterojunction. When a negative voltage is applied to the split gate, the electrons under the gate structure are depleted from the 2DEG and a quasi-one-dimensional (Q1D) device is defined. When the channel length is sufficiently short that electron transport is ballistic, the Q1D constriction exhibits^{2,3} a quantized differential conductance

$$G = n \frac{2e^2}{h}. \quad (1)$$

n is the number of conducting subbands, that is, subbands with energy bottom E_n lower than the Fermi energy E_F , each of which is doubly spin degenerate. As the gate voltage is made more negative the Q1D constriction is narrowed, and E_n changes due to the width of the device and to the change of the potential U_0 at the center of the constriction. When E_n passes through the Fermi energy E_F , the conductance decreases by $2e^2/h$, leading to step-like structure in the conductance versus gate voltage characteristics.

Most transport measurements on such devices have been conducted in the linear-response regime using a small ac voltage (with amplitude less than 0.1 mV) between the source and the drain. When a dc source-drain voltage V_{sd} is applied to the split gate device, the conductance exhibits nonlinear behavior and additional plateaus (called half plateaus) are observed^{4,5} at conductance values midway between those observed in the linear regime. The purpose of this paper is to follow more closely the way in which the half plateaus evolve with increasing V_{sd} . Additionally, we demonstrate a method by which the source-drain voltage can probe the subband energies of a one-dimensional constriction for different gate voltages.

The rest of this paper is organized as follows. In Sec. II we shall describe a simple theory and previous studies.

A theoretical model, based on the work of Büttiker,⁶ incorporating the saddle-point potential and a finite source-drain voltage, have been described more fully elsewhere.⁷ Section III describes the measurement techniques and the samples that were used to obtain the experimental results that are presented in Sec. IV. The various methods by which the subband energy spacings can be determined are discussed in Sec. V. Measurements of the Q1D constriction in a high magnetic field and with an applied source-drain voltage are to be published elsewhere.^{8,9}

II. SIMPLE THEORY AND SUMMARY OF PREVIOUS STUDIES

Many theoretical studies (reviewed in Ref. 10) have investigated the quantization of the conductance in quantum point contacts in the linear-response regime of transport. Models that consider the constriction to be defined by abrupt changes of geometry^{11,12} predict conductance plateaus with resonant structure superimposed on them. To date this resonant structure has not been clearly experimentally observed. Models that consider an adiabatic change in the geometry, predict plateaus in conductance, but not resonant structure on the plateaus. In order to make a more quantitative comparison with the experimental data, the electrostatic potential energy of the narrowest part of the constriction can be approximated by a saddle-point potential.⁶ If the transport between contacts is adiabatic, only the reflection due to the saddle needs to be considered, and can be calculated analytically.¹³

When a dc source-drain voltage V_{sd} is applied to the Ohmic contacts attached to the 2DEG from which the constriction is defined, it is expected that the voltage is dropped predominantly across the high-resistance constriction. To determine the transport properties it is essential to consider how the voltage is dropped between the source and the drain. We define β as the fraction of the dc voltage V_{sd} that is dropped between the source and

the narrowest part of the constriction; therefore the electrochemical potentials at the source and drain are¹⁴

$$\mu_s = E_F + \beta e V_{sd} \quad (2)$$

and

$$\mu_d = E_F - (1 - \beta) e V_{sd}, \quad (3)$$

respectively.

Glazman and Khaetskii (GK) assumed⁴ that $\beta = \frac{1}{2}$ and predicted that, when the source-drain voltage V_{sd} is much smaller than the Fermi energy, $eV_{sd} \ll E_F$, additional plateaus will appear in the differential conductance. If the number n of conducting subbands is large, the additional plateaus (half plateaus) are predicted to be midway between the plateaus given in Eq. (1). For small n some deviations of the conductance from half-integer values could be expected.⁴ The half plateaus appear when the number of conducting subbands for the two directions of transport differs by 1. This prediction was calculated for constrictions defined by smooth geometries. Castaño and Kirczenow¹⁵ calculated the differential conductance of a constriction defined by abrupt changes in the 2DEG, and assuming a linear drop of the dc electrostatic potential in the constriction, they did not find additional plateaus.

Kouwenhoven *et al.*¹⁴ measured the current-voltage (I - V_{sd}) characteristics of a split gate device. The half plateaus were not resolved, but from the onset of nonlinearities in the I - V_{sd} curves, at gate voltage between the $n = 1$ and 2 conductance plateaus, they estimated $\beta \approx \frac{1}{2}$. However, the I - V_{sd} characteristics at gate voltages close to ($n < 1$) and beyond pinchoff gave $\beta \approx 0.2$. Patel *et al.*⁵ presented the first evidence for the appearance of the half plateaus in the differential conductance with an applied source-drain voltage.

III. EXPERIMENTAL DETAILS

The 2DEG formed at the GaAs- $\text{Al}_x\text{Ga}_{1-x}\text{As}$ heterojunction had a mobility $\mu = 10^6$ cm²/V sec and carrier density of 3×10^{11} cm⁻², after illumination with a red light-emitting diode. The Fermi energy E_F is approximately 10 meV. The split gate devices, with a lithographic width and length of 0.3 μm , were similar to those used in a previous study.⁵ The low-temperature measurements were performed in a dilution fridge operating at approximately 40 mK.

A source-drain voltage can be applied across the split gate device in two ways: either by voltage biasing in two-terminal differential conductance G measurements or by current biasing in four-terminal resistance measurements. Four-terminal current biasing measurements eliminate contact resistances and produce more accurate values of the quantized plateaus. However, it is preferable to use voltage biasing because the voltage across the device is independent of the resistance (and hence the gate voltage) of the one-dimensional constriction. The two-terminal technique was used to obtain the results presented in this paper, and the differential conductance

$G = dI/dV_{sd}$ was measured as a function of the dc voltage V_{sd} and the gate voltage V_g . The applied source-drain voltage consisted of an ac and a dc component; the ac component was fixed at an amplitude of 0.1 mV with a frequency of 830 Hz, while the dc component V_{sd} was varied between -10 and $+10$ mV. Modulation techniques were used to enhance the data; for instance, when the gate voltage was swept at different values of V_{sd} , the gate voltage V_g was modulated with an amplitude of 10 mV at a frequency of 31 Hz. Therefore it was possible to measure simultaneously the differential conductance G and the differential transconductance dG/dV_g using two lock-in amplifiers in series tuned at 830 and 31 Hz, respectively. The differential transconductance dG/dV_g is very sensitive to the position of the conductance steps; a peak in dG/dV_g corresponds to a step in the conductance G , and it is possible to measure accurately the gate voltage at which a particular 1D subband is being populated. Measurements of $dG/dV_{sd} = d^2I/dV_{sd}^2$ were made using the $2f$ option on the lock-in amplifier.

As well as the contact resistances of the Ohmic pads, the 2DEG's that exist on either side of the split gate device contribute a resistance that is in series with that of the Q1D constriction. The total resistance (~ 1 k Ω) of these series contributions has been subtracted from the raw data to give the corrected two-terminal conductance shown in the figures. Some of the dc voltage V_{sd} will be dropped across this series resistance, but for the range of gate voltages considered this voltage is small compared to that dropped across the Q1D constriction.

IV. RESULTS

Figure 1 shows gate voltage sweeps of the differential conductance G of a split gate device for fixed values of the source-drain voltage V_{sd} . The left-hand trace was

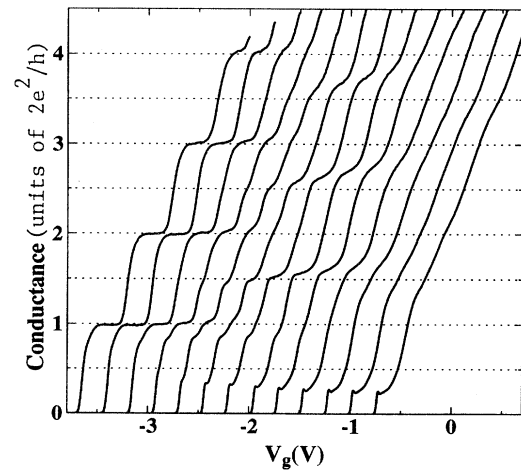


FIG. 1. The differential conductance G vs gate voltage at various source-drain voltages. The successive plots, taken as V_{sd} was incremented in steps of 0.5 mV, have been horizontally offset from each other by 0.2 V from left ($V_{sd} = 0$) to right ($V_{sd} = 6$ mV).

measured at $V_{sd}=0$ and the successive traces, offset to the right for clarity, were measured with V_{sd} incremented in 0.5-mV steps up to 6 mV. When $V_{sd}=0$, the gate voltage sweep exhibits the familiar^{2,3} conductance plateaus quantized in multiples of $2e^2/h$ (integer plateaus). For finite V_{sd} , two types of behavior can be distinguished. First, when the conductance is larger than $2e^2/h$, the integer plateaus become less pronounced as V_{sd} is incremented up to 4 mV, while additional structure (called half plateaus) develops at conductance values approximately midway between the original integer values. At higher source-drain voltages, all the structure becomes smeared out. Second, when the conductance is less than $2e^2/h$, we do not observe voltage-induced structure near e^2/h . Instead, there is weak structure just above $0.8(2e^2/h)$ that weakens at moderate V_{sd} and then disappears when $V_{sd} \approx 4$ mV, and there is a strong feature at $G \approx 0.2(2e^2/h)$ that, in contrast to all the other voltage-induced structure, increases in prominence as the source-drain voltage is increased.

Traces of the differential transconductance dG/dV_g versus the gate voltage V_g , at different source-drain voltages, are shown in Fig. 2. The transconductance is the derivative of the conductance with respect to the gate voltage; therefore, in a gate voltage sweep a zero in the transconductance corresponds to a conductance plateau, and a peak in the transconductance corresponds to the formation of a conductance step. The lowest trace in the figure was measured at $V_{sd}=0$ and successive traces, which are offset in the vertical direction for clarity, show the evolution of the transconductance peaks as the

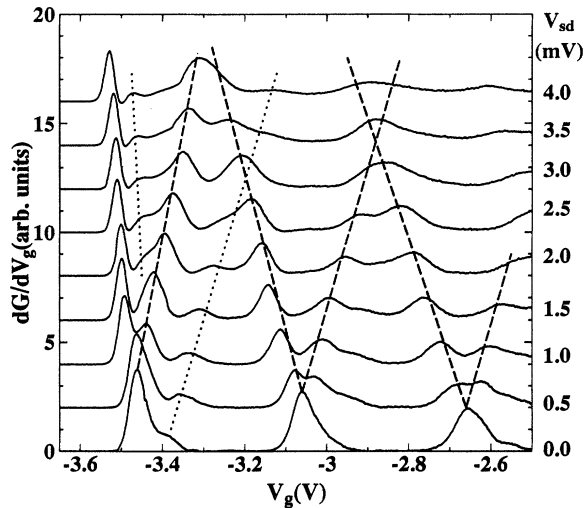


FIG. 2. Traces of the differential transconductance dG/dV_g vs gate voltage for different source-drain voltages. The lowest trace is measured at $V_{sd}=0$, and successive traces (offset in the vertical direction for clarity) show the evolution of the transconductance peaks as V_{sd} is incremented in 0.5-mV steps. As a guide to the eye, the two voltage-induced peaks that are formed from a single peak at $V_{sd}=0$ are marked with dashed lines. Dotted lines show the evolution of two peaks that we were unable to index (see text).

source-drain voltage was increased in 0.5 mV steps. When $V_{sd}=0$ the region of zero transconductance between $V_g \approx -3.35$ and -3.15 V corresponds to the $n=1$ conductance plateau, the region between $V_g \approx -2.9$ and -2.75 V corresponds to the $n=2$ conductance plateau, and for gate voltages less than -3.5 V the device is pinched off. In general, at a given finite source-drain voltage there are twice as many transconductance peaks as there were at $V_{sd}=0$. The two voltage-induced peaks that are formed from the n th peak when $V_{sd}=0$ have been labeled n^+ and n^- according to whether they move to higher or lower gate voltages, respectively. As a guide to the eye, the evolution of the 1^+ , 2^- , 2^+ , 3^- , and 3^+ peaks are followed with dashed lines in Fig. 2, but we were unable to index two peaks, close to the 1^+ and 1^- peaks, whose evolution with V_{sd} are marked with dotted lines. Similar weak satellite peaks were also observed to the right of the 2^+ and 3^+ transconductance peaks, but we were unable to resolve them at finite V_{sd} . The splitting of the n^+ and n^- peaks is linearly dependent on the source-drain voltage, as can be seen more clearly in Fig. 3, where the gate voltages at which the transconductance peaks maxima occur are plotted versus V_{sd} . From a least-squares linear fit to the data points in Fig. 3, we find that the 1^+ and 2^- peaks coincide at 4.5 mV, and the 2^+ and 3^- peaks coincide at 3.2 mV. The same splittings and coincidences were obtained when the polarity of the applied source-drain voltage V_{sd} was reversed.

Traces of the conductance G versus the dc source-drain voltage V_{sd} for different gate voltages are presented in Fig. 4, where the gate voltage has been changed by 0.025 V between each V_{sd} sweep. Lower traces in the figure correspond to gate voltages closer to pinchoff. The data

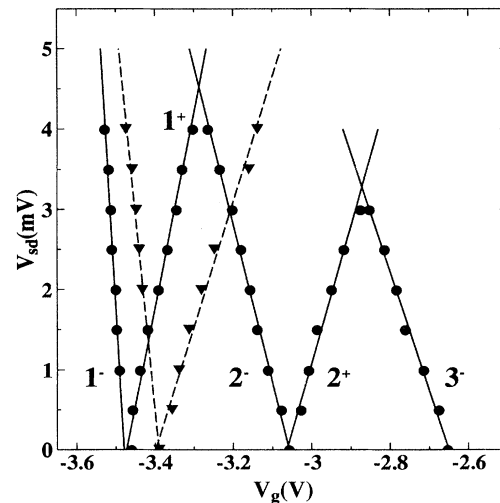


FIG. 3. The variation of the gate voltage positions of the transconductance peaks for the $n=1, 2$, and 3 subbands, as a function of the applied source-drain voltage. The solid lines are the least-squares linear fit to the data points. The variation of the two unindexed peaks are marked by solid triangles, and the fits are shown with dashed lines.

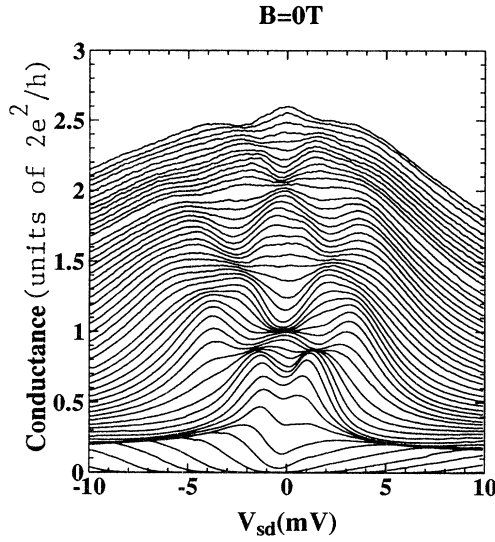


FIG. 4. Traces of the differential conductance G vs the applied source-drain voltage V_{sd} , for different gate voltages V_g . The gate voltage was increased by 0.025 V between successive V_{sd} sweeps.

show a high degree of symmetry when the polarity of the source-drain voltage is reversed, but there is some noticeable asymmetry in the traces close to pinchoff. For some ranges of gate voltage, when V_{sd} is close to zero, the conductance remains approximately constant, and if G were plotted versus gate voltage, this would result in the familiar^{2,3} steplike conductance curves with integer plateaus.

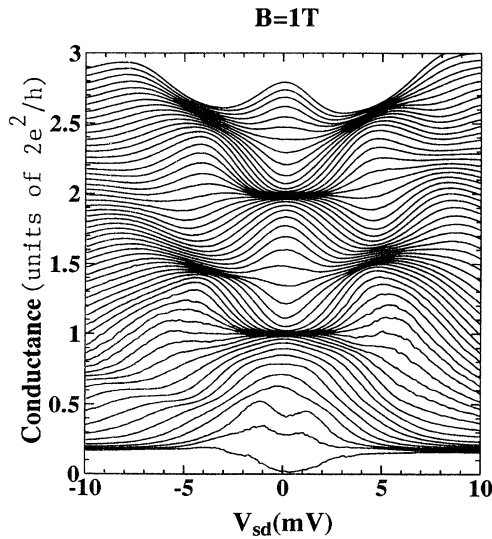


FIG. 5. Traces of the differential conductance G vs the applied source-drain voltage V_{sd} , for different gate voltages. The gate voltage V_g was changed by 0.025 V between successive V_{sd} sweeps. A magnetic field of 1 T was applied perpendicular to the 2DEG.

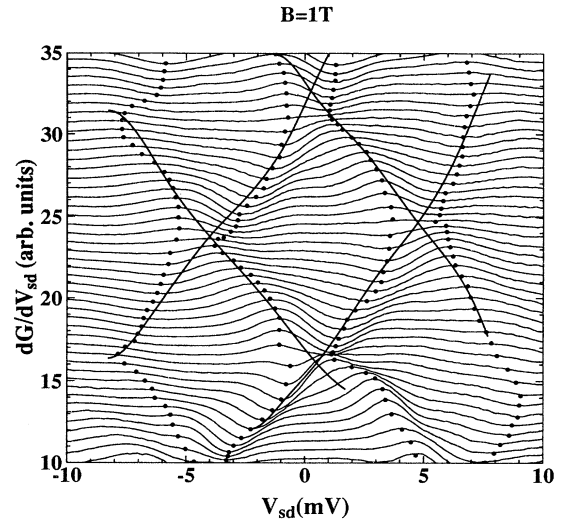


FIG. 6. Traces of $dG/dV_{sd} = d^2I/dV_{sd}^2$ vs the applied source-drain voltage V_{sd} at fixed gate voltage in a perpendicular field of 1 T. The successive traces are offset vertically; the lower the trace, the more negative the gate voltage V_g . The maxima and minima of the dG/dV_{sd} traces are marked with solid bullets, and the solid lines were used to determine V_1 and V_2 .

In source-drain voltage plots such as those shown in Fig. 4, plateaus are represented by a merging of the different traces.

In Fig. 4 there is no indication of a half plateau below $G = 2e^2/h$; instead plateaulike structure is observed at $0.85(2e^2/h)$. For $V_{sd} > 5$ mV the conductance exhibits no further structure and decreases with increasing source-drain voltage. Closer to pinchoff the traces at high V_{sd} merge to a conductance value of $0.2(2e^2/h)$.

The conductance traces in Fig. 5 were obtained under exactly the same experimental conditions as Fig. 4, but in an applied perpendicular field of 1 T. For $G > 2e^2/h$ the plateaus and half plateaus in Fig. 5 are better defined, but qualitatively the same, as those in Fig. 4. For $G < 2e^2/h$ the plateau close to $0.85(2e^2/h)$ has almost disappeared, whereas the structure at $0.2(2e^2/h)$ is unchanged by the magnetic field. An indication of structure close to e^2/h is observed for negative V_{sd} , but not for positive V_{sd} .

The traces of $dG/dV_{sd} = d^2I/dV_{sd}^2$ at fixed gate voltage in a perpendicular field of 1 T are shown in Fig. 6. The successive traces are offset vertically; the lower the trace, the more negative the gate voltage V_g . The position of the maxima and minima in the dG/dV_{sd} traces are marked by solid bullets.

V. DISCUSSION

Due to the different behavior of the conductance for $G > 2e^2/h$ and $G < 2e^2/h$, we will discuss the two cases separately. When $G > 2e^2/h$ the observation of the half-integer conductance plateaus in gate sweeps at fixed V_{sd}

(Fig. 1) and in source-drain voltage sweeps at fixed V_g (Figs. 4 and 5) supports the GK model.⁴ The GK model assumes that half of the source-drain voltage V_{sd} is dropped between the contacts and the bottleneck of the constriction, and predicts that the conductance has the value $(n + 1/2)2e^2/h$ when V_{sd} is such that the number of conducting subbands in the forward and backward directions differs by 1. Comparing Figs. 4 and 5, we see that the integer and half-integer plateaus are better resolved in a moderate perpendicular magnetic field. The magnetic field improves the resolution because it reduces the amount of backscattering from impurities,¹⁶ makes the transport more adiabatic,¹⁷ and narrows the effective width of the channel making the plateaus longer.¹⁸ Figure 5 shows strong evidence that $\beta = \frac{1}{2}$ because the traces originating from the plateaus at $G = (2e^2/h)$ and $2(2e^2/h)$ when $V_{sd} = 0$ merge to form a single structure near $1.5(2e^2/h)$. The half plateaus shown in Fig. 1 drift to conductances that are higher than the expected half-integer values; this could be caused by nonlinearities of the potential drop across the constriction and will be addressed elsewhere.⁷

Theory predicts⁵ that as V_{sd} is increased the half plateaus will be destroyed and integer plateaus will reappear; this occurs when V_{sd} causes the number of conducting subbands in the forward and backward directions to differ by 2. The reappearance of the integer plateaus was not observed when $B = 0$ because the conductance of all traces in Fig. 4 (except those close to pinchoff) decrease monotonically for $V_{sd} > 4$ mV. We associate this rolloff in the conductance with the transport being no longer ballistic, due to a decrease of the inelastic mean free path caused by the source-drain voltage. In the presence of a perpendicular magnetic field, see Fig. 5, the reappearance of the integer plateaus at $G \approx 2(2e^2/h)$ when $V_{sd} = \pm 8$ mV shows the increase of the mean free path by a perpendicular magnetic field, as observed¹⁹ for $V_{sd} = 0$. Our observation of ballistic effects for source-drain voltages up to 10 mV in a small perpendicular magnetic field is in agreement with the electron focusing experiments of Williamson *et al.*²⁰

The formation of the half plateaus from the integer plateaus with increasing V_{sd} can be clearly followed in the transconductance traces in Fig. 2. The linear evolution of the half plateaus indicates that the energy difference $E_F - E_n$ between the bottom of a given subband at the bottleneck of the constriction and the Fermi energy varies linearly with gate voltage V_g . The left-hand side of each transconductance peak is associated with the case where E_F is just less than E_n , and the electrons can tunnel through the constriction. The right-hand side corresponds⁶ to quantum reflection of the electrons when E_F is just greater than E_n . While the left-hand side of the transconductance peaks measured at $V_{sd} = 0$ can be fitted to the shape predicted by theory,⁶ we are unable to explain how the right-hand structure arises.

From the effect of the source-drain voltage on the differential conductance for $G > 2e^2/h$ it is possible to extract the energy spacing between the n and $n + 1$ subbands of the Q1D constriction $\Delta E(n, n + 1) = E_{n+1} - E_n$.

Early measurements^{21,22} of $\Delta E(n, n + 1)$ were indirectly made from the depopulation of the Q1D subbands by a perpendicular magnetic field, and fitting the results with a parametrized model of the confining potential. Kouwenhoven *et al.*¹⁴ in their study of the $I-V_{sd}$ characteristics determined $\Delta E(1, 2)$ from the maximum source-drain voltage of the onset of nonlinear behavior on the $n = 1$ conductance plateau. The method we used previously⁵ relied on a similar technique. These methods are valid only at certain gate voltages, whereas a method proposed by Zagoskin²³ allows $\Delta E(n, n + 1)$ to be determined for any gate voltage. The latter method is based on the idea that, as the source-drain voltage is increased, the subbands are populated and depopulated giving rise to a conductance that switches between integer and half-integer values. Assuming that half of the applied source-drain voltage V_{sd} is dropped between the contacts and the center of the constriction, and that $E_{n+1} > E_F > E_n$, the subband energy spacing at fixed gate voltage is²³

$$\Delta E(n, n + 1) = \frac{e}{2}(V_1 + V_2), \quad (4)$$

where V_1 is the source-drain voltage at which the first extremum in d^2I/dV_{sd}^2 occurs, and V_2 is the voltage of the second extremum. For Eq. (4) to be valid, if V_1 is a maximum, V_2 must be a minimum, and vice versa. The data in Fig. 6 were obtained in a perpendicular magnetic field of 1 T, and the positions of the extrema are marked with solid bullets on the d^2I/dV_{sd}^2 traces. The solid lines in Fig. 6 are an extrapolation of the well-resolved extrema to the region where a clear distinction is not possible. The traces that show a small value of V_1 and a large value of V_2 correspond to gate voltages where E_F is close to the bottom of one of the subbands. The traces for which V_1 and V_2 are similar correspond to the case when E_F is approximately midway between E_n and E_{n+1} .

The subband energy spacing $\Delta E(1, 2)$ as a function of gate voltage is plotted in Fig. 7, as obtained from the data of Fig. 6 using Eq. (4). The solid bullets show the values of $\Delta E(1, 2)$ obtained from the resolved extrema and the extrapolated lines in Fig. 6. The data show that

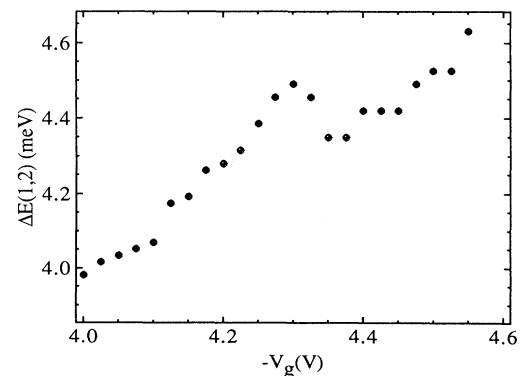


FIG. 7. Subband energy spacing $\Delta E(1, 2)$ as function of gate voltage, determined from Fig. 6 using the method of Zagoskin (Ref. 23).

$\Delta E(1,2)$ is an insensitive function of gate voltage. Therefore the main effect of the gate voltage is to change the potential U_0 at the center of the constriction, rather than reducing the width of the constriction.

In zero magnetic field, the conductance traces roll off obscuring the position of V_2 and it is not possible to obtain the subband energy spacings for general gate voltage. However, when the n^+ and $(n+1)^-$ transconductance peaks coincide $V_1=V_2$, in which case Eq. (4) becomes $\Delta E(n, n+1)=eV_1$, and the subband energy spacing is determined only at the gate voltage of coincidence. The values $\Delta E(1,2)=4.5$ meV and $\Delta E(2,3)=3.2$ meV are obtained from Fig. 3. This method of measuring $\Delta E(n, n+1)$ is similar to that used previously,^{5,14} but is a special case of the more general method proposed by Zagoskin.²³

For $G < 2e^2/h$ there is no half plateau. Instead, the gate sweeps in Fig. 1 show structure at conductances of $0.2(2e^2/h)$ and $0.8(2e^2/h)$. The simultaneous observation of plateaus at $0.2(2e^2/h)$ and $0.8(2e^2/h)$ cannot be explained using the GK model. On one hand, if $\beta=0.2$, then plateaus are expected at $0.4(2e^2/h)$ and $0.6(2e^2/h)$, as well as at $0.2(2e^2/h)$ and $0.8(2e^2/h)$. On the other hand, if $\beta=0.8$, no extra plateaus are expected⁷ below $0.8(2e^2/h)$. The structure close to $0.8(2e^2/h)$ is qualitatively similar to the half-integer plateaus; the structure becomes well defined at moderate source-drain voltage $V_{sd} \approx 2$ mV, and then disappears at higher voltages.

The structure that is observed in the last conductance step near $0.8(2e^2/h)$ at $V_{sd}=0$ has been observed by others,²² but its presence passed without comment. In Fig. 2, the transconductance peak associated with this structure, close to the $n=1$ peak, separates from the transconductance peak labeled 1^+ as V_{sd} is increased. The gate voltage positions of this transconductance peak, as well as the position of the peak associated with the structure at $0.2(2e^2/h)$, have been plotted in Fig. 3 with dashed

lines. The splitting of these unindexed peaks as V_{sd} is increased is similar to the splitting of the 1^+ and 1^- peaks; however, the two pairs of peaks behave independently. The origin of the unindexed peaks and their development with V_{sd} is not understood at the moment.

VI. CONCLUSIONS

The adiabatic model of Glazman and Khaetskii⁴ predicts the manner in which an applied source-drain voltage V_{sd} is dropped across the quasi-one-dimensional constriction. We have presented measurements that support the GK model, and show that the phenomenological parameter is $\beta \approx \frac{1}{2}$ for subband indices $n > 1$. In this study we observe a linear development of the splitting of the transconductance peaks with an applied source-drain voltage. In a small perpendicular magnetic field, $\Delta E(1,2)$ has been determined for a range of gate voltages by looking at the structure in dG/dV_{sd} as a function of V_{sd} and V_g . For zero magnetic field, adjacent transconductance peaks in gate voltage sweeps coincide when $eV_{sd}=\Delta E(n, n+1)$; however this subband energy spacing is determined only at the gate voltage of coincidence.

For $G < 2e^2/h$ no half plateau is observed. Instead there is anomalous structure at $0.2(2e^2/h)$ and $0.8(2e^2/h)$, which also shows linear splittings as the source-drain voltage is increased.

ACKNOWLEDGMENTS

This work was supported by the SERC and by the EEC under the auspices of ESPRIT Basic Research Action 3043, and also by the European Research Office of the U.S. Army. J.T.N. acknowledges support from the Leverhulme Trust and the I. Newton Trust, and L.M.M. acknowledges support from Spain's Ministerio de Educación y Ciencia.

¹T. J. Thornton, M. Pepper, H. Ahmed, D. Andrews, and G. J. Davies, Phys. Rev. Lett. **56**, 1198 (1986).

²B. J. van Wees, H. van Houten, C. W. J. Beenakker, J. G. Williamson, L. P. Kouwenhoven, D. van der Marel, and C. T. Foxon, Phys. Rev. Lett. **60**, 848 (1988).

³D. A. Wharam, T. J. Thornton, R. Newbury, M. Pepper, H. Ahmed, J. E. F. Frost, D. G. Hasko, D. C. Peacock, D. A. Ritchie, and G. A. C. Jones, J. Phys. C **21**, L209 (1988).

⁴L. I. Glazman and A. V. Khaetskii, Europhys. Lett. **9**, 263 (1989).

⁵N. K. Patel, L. Martín-Moreno, M. Pepper, R. Newbury, J. E. F. Frost, D. A. Ritchie, G. A. C. Jones, J. T. M. B. Janssen, J. Singleton, and J. A. A. J. Perenboom, J. Phys.: Condens. Matter **2**, 7247 (1990).

⁶M. Büttiker, Phys. Rev. B **41**, 7906 (1990).

⁷L. Martín-Moreno, J. T. Nicholls, N. K. Patel, and M. Pepper (unpublished).

⁸N. K. Patel, L. Martín-Moreno, J. T. Nicholls, M. Pepper, J. E. F. Frost, D. A. Ritchie, and G. A. C. Jones, Superlatt. Mi-

crostruct. (to be published).

⁹N. K. Patel, J. T. Nicholls, L. Martín-Moreno, M. Pepper, J. E. F. Frost, D. A. Ritchie, and G. A. C. Jones, Phys. Rev. B **44**, 10973 (1991).

¹⁰C. W. J. Beenakker and H. van Houten, *Solid State Physics* (Academic, New York, 1990), Vol. 44.

¹¹A. Szafer and A. D. Stone, Phys. Rev. Lett. **62**, 300 (1989).

¹²G. Kirczenow, Solid State Commun. **68**, 715 (1988).

¹³H. A. Fertig and B. I. Halperin, Phys. Rev. B **36**, 7969 (1987).

¹⁴L. P. Kouwenhoven, B. J. van Wees, C. J. P. M. Harmans, J. G. Williamson, H. van Houten, C. W. J. Beenakker, C. T. Foxon, and J. J. Harris, Phys. Rev. B **39**, 8040 (1989).

¹⁵E. Castaño and G. Kirczenow, Phys. Rev. B **41**, 3874 (1990).

¹⁶M. Büttiker, Phys. Rev. B **38**, 9375 (1988).

¹⁷L. I. Glazman and M. Jonson, J. Phys. Condens. Matter **1**, 5547 (1989).

¹⁸K.-F. Berggren, T. J. Thornton, D. J. Newson, and M. Pepper, Phys. Rev. Lett. **57**, 1769 (1986).

¹⁹B. W. Alphenaar, P. L. McEuen, R. G. Wheeler, and R. N.

- Sacks, Phys. Rev. Lett. **64**, 677 (1990).
- ²⁰J. G. Williamson, H. van Houten, C. W. J. Beenakker, M. E. I. Broekaart, L. I. Spendeler, B. J. van Wees, and C. T. Foxon, Phys. Rev. B **41**, 1207 (1990).
- ²¹D. A. Wharam, U. Ekenberg, M. Pepper, D. G. Hasko, H. Ahmed, J. E. F. Frost, D. A. Ritchie, D. C. Peacock, and G. A. C. Jones, Phys. Rev. B **39**, 6283 (1989).
- ²²B. J. van Wees, L. P. Kouwenhoven, H. van Houten, C. W. J. Beenakker, J. E. Mooij, C. T. Foxon, and J. J. Harris, Phys. Rev. B **38**, 3625 (1988).
- ²³A. M. Zagoskin, Pis'ma Zh. Eksp. Teor. Fiz. **52**, 1043 (1990) [JETP Lett. **52**, 435 (1991)].